

Evaporative cooling of highly charged dysprosium ions in an enhanced electron-beam ion trap

B. M. Penetrante, J. N. Bardsley, M. A. Levine, D. A. Knapp, and R. E. Marrs

High Temperature Physics Division, Lawrence Livermore National Laboratory, Livermore, California 94550

(Received 19 December 1990)

The mechanism of evaporative cooling of highly charged ions in an electron-beam ion trap (EBIT) is discussed. Computer simulations of evaporative cooling in superEBIT indicate that with the use of neon, nitrogen, or helium coolants, significant amounts of bare and hydrogenlike dysprosium ions can be trapped indefinitely for the observation of bound-state β decay.

I. INTRODUCTION

The electron-beam ion trap (EBIT) is an instrument designed for the study of very highly charged ions.¹⁻⁴ Ionization stages of almost any element in the Periodic Table can be produced and trapped for several hours. The most highly charged ion studied in the EBIT to date is neonlike uranium U^{82+} . In the EBIT, an electron beam serves to electrostatically trap the ions, strip partially ionized atoms to create highly charged ions, and probe these ions for *in situ* study. The EBIT is capable of preselecting an ionization stage with one-electron energy and probing it with another. Combined with a spectrometer for obtaining high-resolution x-ray spectra,⁵ the EBIT can be used to perform many types of measurements that have not been possible before.⁶⁻¹⁰

Currently under construction is an enhanced version of the EBIT, called superEBIT, that will have electron energies up to 150 keV, enough to ionize any element completely.¹¹ One of the experiments to be done on the superEBIT is the observation of bound-state β decay.¹² Bound-state β decay is a process in which an electron is created in a vacant bound atomic state. A few normally stable isotopes undergo nuclear decay when their atomic electrons are removed. The most promising isotope for observing this effect in the superEBIT is ^{163}Dy . Normally, ^{163}Ho decays by electron capture into ^{163}Dy ; however, when electrons are removed from the inner shells of ^{163}Dy , it can decay back into ^{163}Ho . The half-life for totally bare Dy is estimated to be about 37 days, with a decay energy of 50 keV for orbital insertion into the *K* shell. To observe this mode of nuclear decay, fully stripped Dy ions will have to be trapped at low energy for several hours. In the trap the ions can be continuously observed by detecting their characteristic x rays.

In the absence of cooling, the collisional heating of the ions by the electron-beam limits the maximum charge state and the time that the ions can remain trapped. However, the ions can be cooled by continuous injection of low-*Z* atoms into the trap. In this paper we present calculations that show the importance of various processes on the selection of these atoms. These calculations are done to attempt to optimize the cooling process. We deal specifically with maximizing the number of trapped bare Dy ions in the superEBIT. The information we provide is valuable to other EBIT systems as well.

II. EVAPORATIVE COOLING IN THE EBIT

The design and operation of the EBIT has been described in detail elsewhere.^{1,2} A schematic of the operation of the EBIT is shown in Fig. 1. The trap consists of an electron beam that passes through a series of three drift tubes. The electron beam is compressed to current densities of up to 6000 A/cm^2 by the 3-T field of two superconducting Helmholtz coils. Ions are trapped radially by a combination of the space charge of the electron beam and the applied axial magnetic field. Axial trapping is provided by potentials applied to the end drift tubes. The central drift tube has an inside diameter of 10 mm over a length of 20 mm. The ions are continually ionized by collisions with beam electrons. The collisions also excite x rays, allowing the ions to be observed *in situ*. The ions are injected into the trap either as a neutral gas or as low-charge ions from a metal vapor vacuum arc source.¹³

Simple calculations would indicate that heating of the ions from electron-ion collisions limits the highest charge

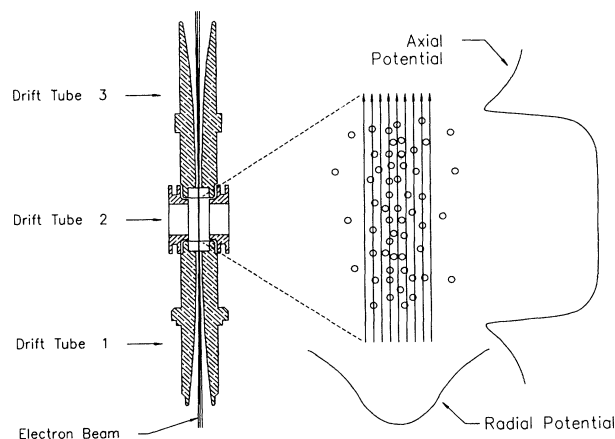


FIG. 1. Schematic of the EBIT operation. A high-current-density electron beam passes through three drift tubes. Ions are trapped radially by a combination of the electron-beam space charge and an axial magnetic field. Axial trapping is provided by voltages applied to drift tubes 1 and 3. Collisions with the beam electrons ionize the ions and excite x rays, which are viewed at 90° through viewports in drift tube 2.

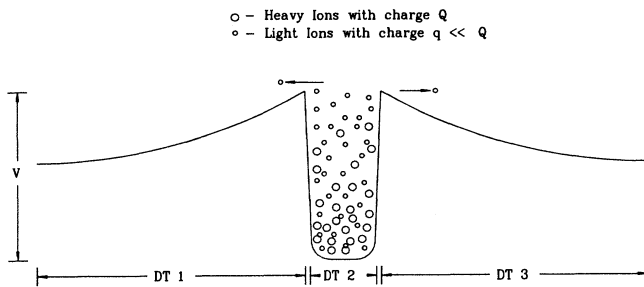


FIG. 2. Evaporative cooling in the EBIT. High-charge ions are trapped by a potential of QV , while low charge ions only by qV . The temperature of all ions equilibrates through ion-ion collisions. The low-charge ions preferentially escape, cooling the high-charge ions.

state attainable in the EBIT to $q_{\max} = +40$, but it was discovered that the ions can be cooled by continuous injection of low- Z atoms into the trap.^{1,2} The cooling results in dramatic improvements in ion density, ultimate charge state, and trapping time. Figure 2 is an illustration of the evaporative cooling process. The trapping potential for an ion of charge state q is qV , where V is the voltage applied to the end drift tubes. Ions with a higher kinetic energy will escape the trap. The ion-ion collision rates in the trap are very high, so the temperature of all the ions remains near equilibrium. Therefore, when a constant flux of low- Z ions is added to the trap, they will preferentially escape, cooling the high- Z ions. The scheme has proven remarkably successful. Schneider *et al.*¹⁴ have demonstrated the effectiveness of evaporative cooling in a measurement of the containment time of neonlike gold Au^{69+} cooled by titanium. In their experiment, an exponential decay time of 4.5 h for neonlike gold ions was observed. Neutral nitrogen gas has also been used as a coolant and trapping times in excess of 5 h have been observed.

The highest ionization state present in the trap is determined by the electron-beam energy. For example, a minimum beam energy of 63.1 keV is required to fully ionize Dy ($Z=66$). The detailed ionization balance is determined by the relative rates of ionization and recombination. The theoretical limit on the ionization balance is determined by the ratio of two electron-ion interactions: impact ionization and radiative recombination. However, there is also an unavoidable contribution from charge exchange with neutral atoms and low-charge-state ions. The low- Z material used to cool the high- Z ions in the trap must be selected carefully to provide adequate cooling while not significantly degrading the charge-state balance through charge exchange.

III. COMPUTER SIMULATION OF THE EBIT

We have developed a code to calculate the evolution of the ion charge-state distribution in an electron-beam ion trap. The code solves the set of coupled nonlinear rate equations for the ion number and energy balance. Code inputs are the neutral gas density of the coolant, initial total density of the injected high- Z ions, electron-beam

energy and current, applied axial potential, magnetic field strength, physical dimensions of the trap, and atomic physics data. Details of the calculations are described by Penetrante *et al.*¹⁵

The processes controlling the ion number balance are (i) electron-impact ionization, (ii) radiative recombination, (iii) charge exchange, and (iv) radial and axial ion escape from the trap. The processes controlling the energy balance are (i) heating of the ions by the electron beam, (ii) energy transfer among the individual ions, and (iii) energy loss through radial and axial ion escape. The effective radial potential is calculated from the combined effects of the electron-beam space charge (given by the beam energy and current) and the magnetic field (3 T). We assume that the electron beam is operating with an energy of 150 keV and a current of 150 mA. The beam radius is around $33 \mu\text{m}$. Axial trapping is provided by an applied potential well (varied between 100 and 300 V), which we assume to be a square well. For the ionization cross sections we use the formula derived by Lotz.¹⁶ The radiative-recombination cross section derived by Kim and Pratt¹⁷ is used. The charge-exchange cross section formula is given by Müller and Salzborn.¹⁸ The electron-ion and ion-ion energy exchange rates are derived from the Coulomb collision rates.^{19,20} The electron-ion and ion-ion rates depend on the electron-beam-ion and ion-ion overlaps, respectively. We approximate these overlap factors by the overlap in the volumes occupied by the ions. When the ions get heated they spend part of their time outside the beam and eventually escape out of the trap when their energies exceed the trapping potential. The ion escape rate is obtained from an approximate solution of the Fokker-Planck equation.²¹

Dy is injected as a pulse of low-charged ions. The coolant is continuously introduced into the trap ballistically perpendicular to the electron beam. Our aim is to find the set of operating parameters that will maximize the number of trapped totally bare Dy ions and their trapping time. By operating parameters we mean (i) the type of coolant, (ii) the density of the coolant intersecting with the beam, (iii) the total number of Dy ions initially injected into the trap, and (iv) the axial potential well depth.

IV. RESULTS

For the purpose of observing bound-state β decay, we desire as large a fraction as possible of bare and H-like Dy. The higher the beam energy, the better. The superEBIT will initially have a maximum beam energy of 150 keV. Figure 3 shows the time evolution of the Dy ion charge-state distribution at 150 keV in the idealized case in which the charge balance is determined only by ionization and radiative recombination. In this calculation the amount of background gas that can cause ion depletion as a result of charge exchange is assumed to be negligible. The effect of ion heating by the electron beam is not taken into account. Thus it is assumed that all the ions are within the electron beam and eternally confined within the trap. The maximum fraction of Dy^{66+} ions is about 7%. This is fixed by the ratios of the radiative-

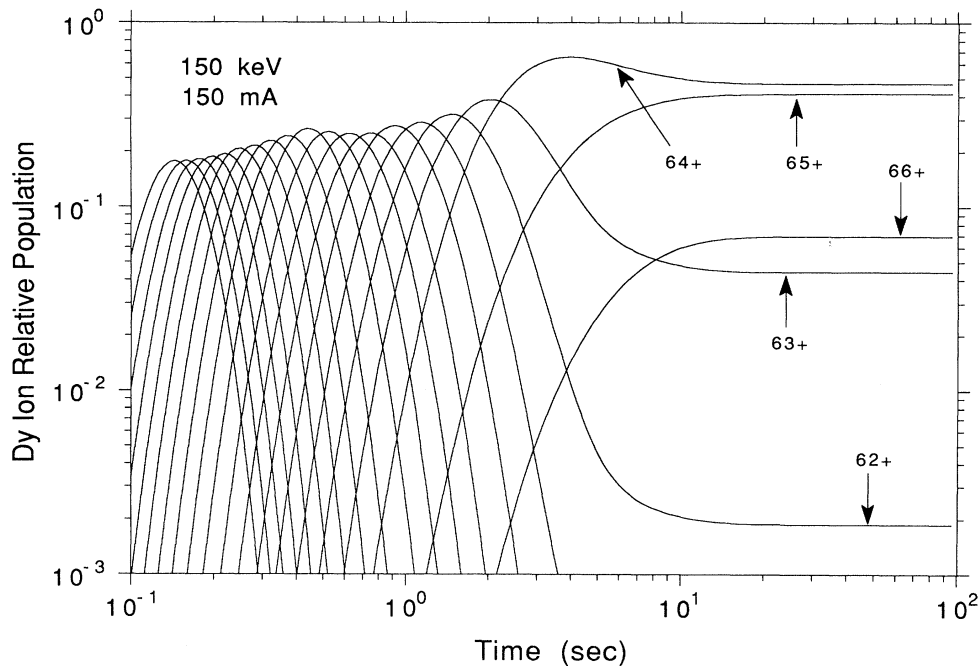


FIG. 3. Evolution of the Dy ions in the idealized case in which the charge balance is determined only by ionization and radiative recombination. ($E_e = 150$ keV, $I = 150$ mA, $B = 3$ T.)

recombination cross section to the ionization cross section.

The total number of Dy ions injected into the trap must be chosen so that the ion space charge does not significantly neutralize the electron space charge. This provides for the best radial trapping and the best effective ionization rates. If we assume that the Dy ions are cool enough to be within the beam, then we can easily estimate this total amount of Dy ions based on the charge state distribution in Fig. 3 and the level of neutralization we are willing to tolerate. For an electron beam of 150 keV and 150 mA, the electron density is about 10^{12} cm^{-3} . The Dy ions consist of 4.5% Dy^{63+} , 47% Dy^{64+} , 41% Dy^{65+} , and 7% Dy^{66+} . Thus for a beam neutralization of 5%, the total density of the Dy ions is about 10^9 cm^{-3} . This total density determines the total number of Dy ions that is injected into the trap. In the following we take this to be the total Dy ion density and concentrate on the coolant parameters. A 5% beam neutralization yields a number of highly charged ions close to that observed experimentally in the EBIT.

Figure 4 compares the effectiveness of different coolants in reducing the Dy ion temperatures, using the same neutral coolant density of 10^4 cm^{-3} . The Dy ions gain energy from the electron beam. This energy, or part of it, is transferred to the coolant ions, and the coolant ions escape out of the trap faster because of their smaller charge, thus effectively cooling the Dy ions. Only the Dy^{66+} ion temperature is shown in the figure; the other highly charged Dy ions have temperatures very close to it because of the strong energy coupling among these ions. The energy carried out by each escaping coolant ion is approximately proportional to its charge. For the same

number of atoms, the heavier coolants take out more energy per atom.

The heavier coolants have the advantage of carrying away more energy for each escaping ion because they can reach higher charge states. However, they also have a disadvantage because the additional trapping time of the more highly charged coolant ions greatly increases their

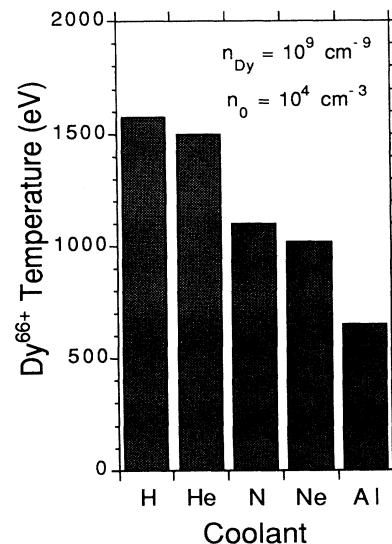


FIG. 4. Temperature of the Dy^{66+} ion for various coolants. The neutral density is 10^4 cm^{-3} and the initial total Dy ion density is 10^9 cm^{-3} . ($E_e = 150$ keV, $I = 150$ mA, $V_w = 300$ V, $B = 3$ T.)

density within the electron beam. Thus the heavier coolants are more likely to encounter limitations from neutralization of the electron-beam space charge. Figure 5 shows the maximum neutral density for different coolants to neutralize about 10% of the electron-beam space charge. We use these densities as limiting values that will provide for the lowest Dy ion temperatures without overly degrading the radial confinement.

Figure 6 shows the steady-state charge-state density distribution of the trapped Dy ions for different coolants at the limiting density. The initial total density of Dy ions is 10^9 cm^{-3} ; however, some of the Dy ions escape whenever there is insufficient cooling. The axial trapping potential is fixed at 300 V. The best Dy charge-state distributions are achieved with neon, nitrogen, and helium. Hydrogen is not an effective coolant because the energy removed per ion is small and the charge-exchange cross section is large. Aluminum suffers from a large charge-exchange rate even at the low densities required to cool the Dy^{66+} . Neon results in the best charge-state distribution for Dy. It is the most desirable because (i) it provides coolant ions with charge states high enough to be highly effective in carrying energy out of the trap, and (ii) it has a small charge-exchange cross section because of its large neutral ionization potential.

Figure 7 shows the steady-state values of the effective rates of the highly charged Dy ions for a neon coolant with a neutral density of 10^4 cm^{-3} . At steady state, the sum of the radiative-recombination and charge-exchange rates for each charge state is equal to the ionization rate

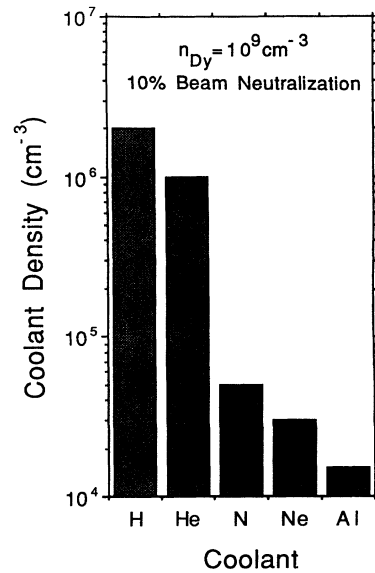


FIG. 5. Neutral coolant density, chosen such that the coolant ions neutralize about 10% of the electron-beam space charge. The initial total Dy ion density is 10^9 cm^{-3} . ($E_e = 150 \text{ keV}$, $I = 150 \text{ mA}$, $V_w = 300 \text{ V}$, $B = 3 \text{ T}$.)

of the next lower charge state. Note that the charge-exchange rates are much smaller than the radiative-recombination rates for all the Dy charge states. Thus the Dy ion charge-state distribution attained with neon is

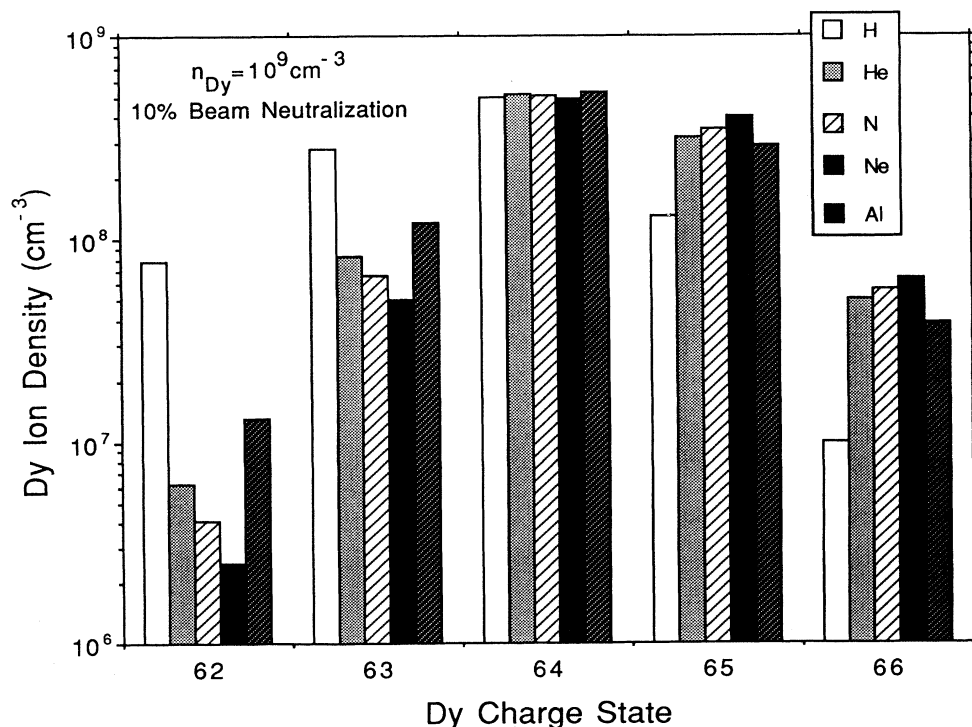


FIG. 6. Charge-state density distribution of the Dy ions for various coolants. The initial total Dy ion density is 10^9 cm^{-3} . The coolant density is chosen such that the coolant ions neutralize about 10% of the electron-beam space charge. ($E_e = 150 \text{ keV}$, $I = 150 \text{ mA}$, $V_w = 300 \text{ V}$, $B = 3 \text{ T}$.)

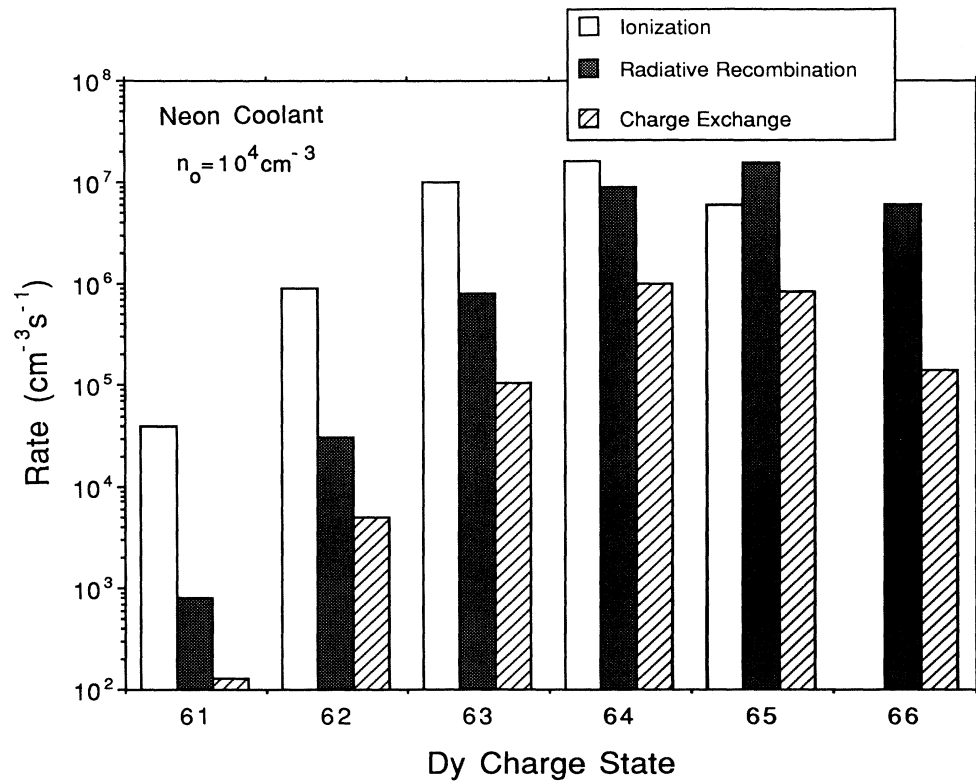


FIG. 7. Effective rates of the highly charged Dy ions for a neon coolant with a neutral density of 10^4 cm^{-3} . The initial total Dy ion density is 10^9 cm^{-3} . ($E_e = 150 \text{ keV}$, $I = 150 \text{ mA}$, $V_w = 300 \text{ V}$, $B = 3 \text{ T}$.)

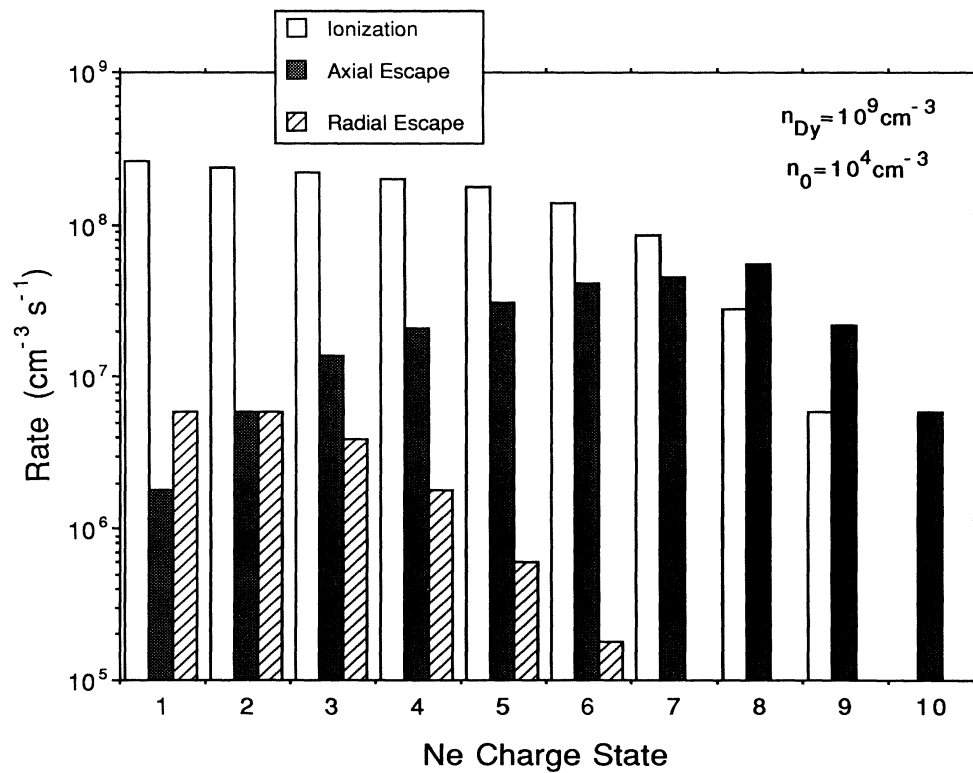


FIG. 8. Effective rates of the neon coolant ions. The neutral neon density is 10^4 cm^{-3} and the initial total Dy ion density is 10^9 cm^{-3} . ($E_e = 150 \text{ keV}$, $I = 150 \text{ mA}$, $V_w = 300 \text{ V}$, $B = 3 \text{ T}$.)

close to the ideal case.

Figure 8 shows the steady-state values of the effective ionization, axial escape, and radial escape rates of the neon coolant ions. The conditions are the same as in Fig. 7. The lower-charged ions are loosely bound to the electron beam, and therefore a significant amount of radial escape takes place for these ions. The higher charged

ions escape only axially. Radiative recombination and charge exchange contribute negligible amounts to the charge balance of the coolant ions.

Figure 9(a) shows the evolution of the Dy ion charge-state density distribution when using a neon coolant with a neutral density of 10^4 cm^{-3} . The steady-state distribution is very close to the ideal case (see Fig. 3); however, it

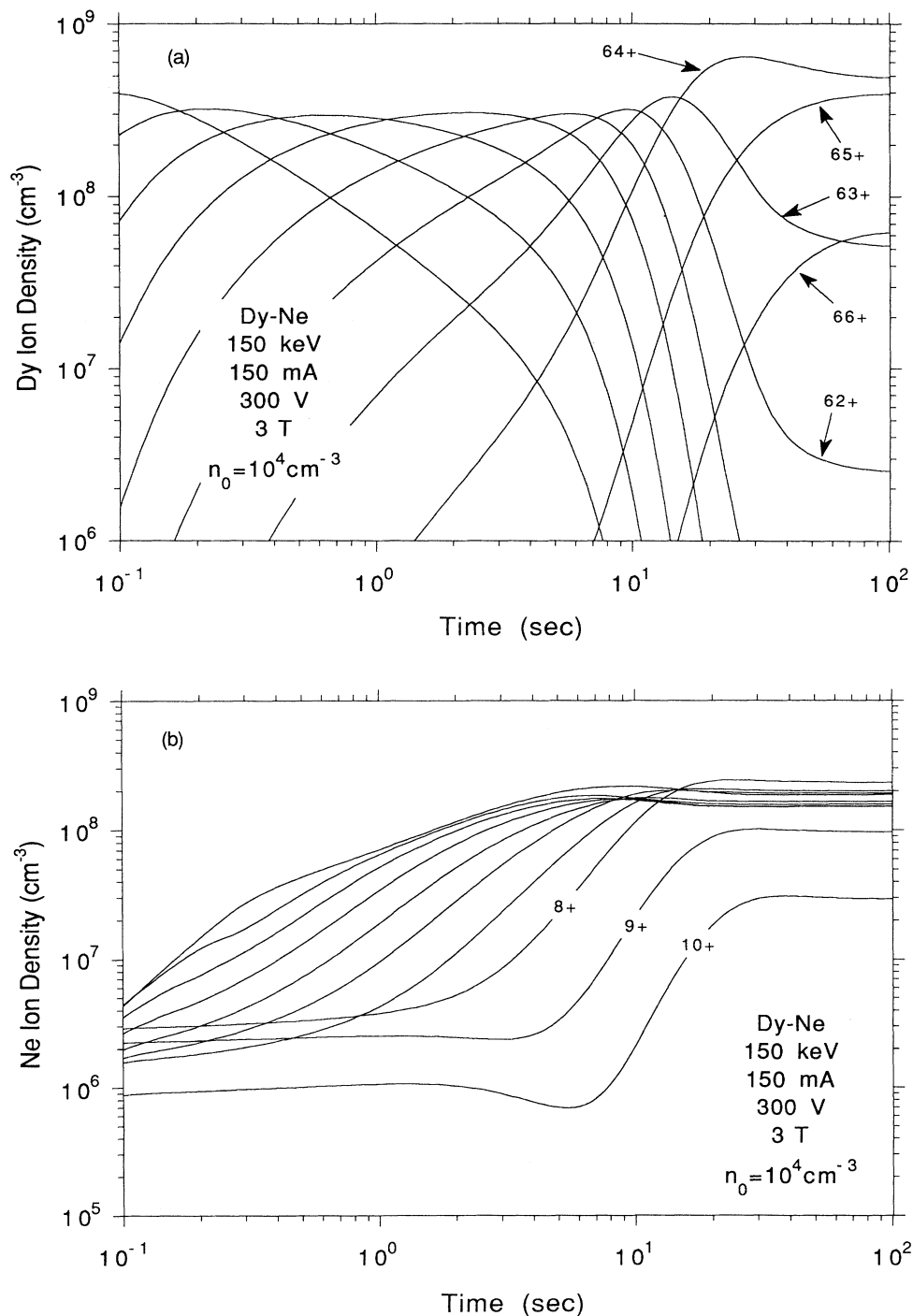


FIG. 9. Evolution of the charge-state density distributions of the (a) Dy ions and (b) neon coolant ions. The neutral neon density is 10^4 cm^{-3} and the initial total Dy ion density is 10^9 cm^{-3} . ($E_e = 150 \text{ keV}$, $I = 150 \text{ mA}$, $V_w = 300 \text{ V}$, $B = 3 \text{ T}$.)

takes 100 sec (as opposed to 10 sec) to reach it. The time to steady state depends on the amount of coolant used because the effective ionization rates depend on the electron-ion overlap factors, which in turn depend on the ion temperatures. Since in the β -decay experiment the Dy ions will be trapped for many hours, it is not relevant how quickly they achieve a steady-state distribution. The crucial concern is that the coolant ions carry away all the energy the Dy ions absorb from the electron beam, so that all the Dy ions that were injected remain trapped. Figure 9(b) shows the corresponding evolution of the neon ions. Note the large proportion of low-charged neon ions. Most of the cooling is distributed among ionization states from Ne^{4+} to Ne^{9+} .

Figure 10 shows the effect of excessive cooling on the evolution of the charge-state distribution of the neon ions. A neutral neon density of 10^4 cm^{-3} is sufficient to provide adequate cooling for the Dy ions. Any additional cooling traps the most highly charged coolant ions as well. Note the large amounts of Ne^{8+} to Ne^{10+} . These high-charge coolant ions neutralize the electron beam, reducing the radial trapping potential. The density of the lower-charged neon ions decreases because of the decreasing effective ionization rate (decreasing electron-ion overlap). Because of the neutralization caused by the coolant ions, the Dy ions spend less time in the beam and the charge balance is degraded by charge exchange outside the beam.

Figure 11 shows the effect of reducing the axial potential well on the charge-state distribution of the neon ions. An axial potential well of 100 V is not deep enough to

trap the higher-charged coolant ions long enough to absorb energy from the Dy ions. Because of the small amounts of higher-charged coolant ions the effectiveness of neon is lost. Not enough cooling of the Dy ions takes place and a significant amount of Dy is lost through axial escape. The density of Ne^{8+} eventually gets high, as shown in Fig. 11, but by then significant amounts of Dy ions have already escaped. Increasing the amount of coolant will not remedy the situation since charge exchange would then degrade the Dy charge-state distribution.

Figure 12 shows the time evolution of the ion temperatures for the operating parameters that provide optimum cooling. The temperatures increase monotonically until around 2 sec. Afterwards the temperatures of the higher-charged ions decrease before leveling off to their steady-state values. The existence of the overshoot in the temperature evolution is caused by the finite time required to produce significant amounts of Ne^{7+} , Ne^{8+} , and Ne^{9+} ions that efficiently cool the highly charged Dy ions.

V. DISCUSSION

The theoretical Dy^{66+} densities attained using He through Al are within the accuracy of the cross sections used in the calculations. These calculations are particularly sensitive to the ionization cross sections. The densities of the coolants shown in Fig. 5 are inversely proportional to the cross section for ionization of the neutral species. The neutral density used determines the rate of

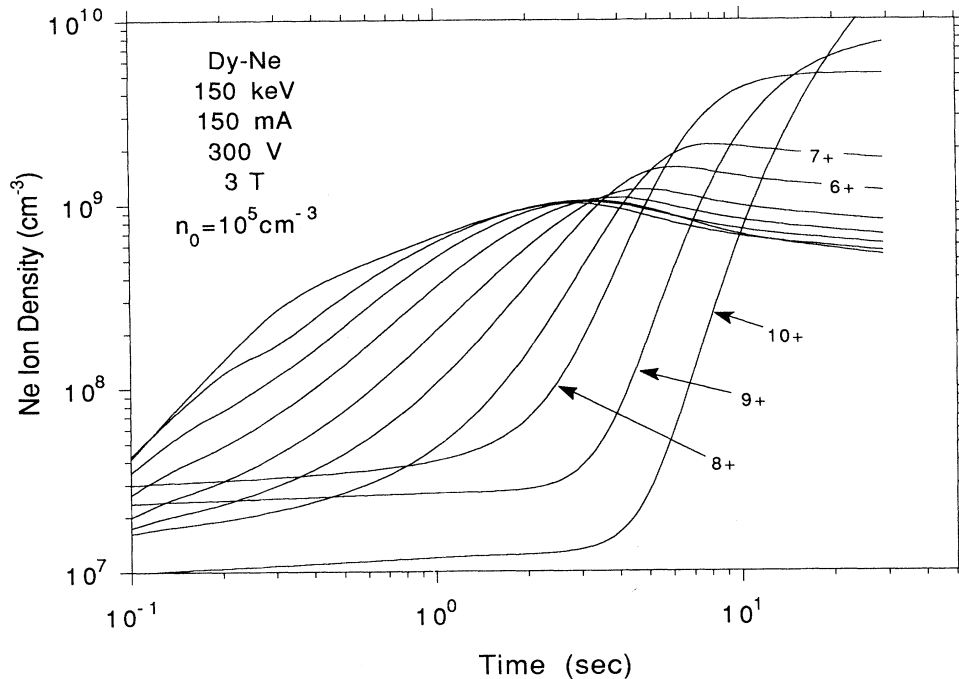


FIG. 10. Effect of overcooling on the charge-state distributions of the neon coolant ions. The neutral neon density is 10^5 cm^{-3} and the initial total Dy ion density is 10^9 cm^{-3} . ($E_e = 150 \text{ keV}$, $I = 150 \text{ mA}$, $V_w = 300 \text{ V}$, $B = 3 \text{ T}$.)

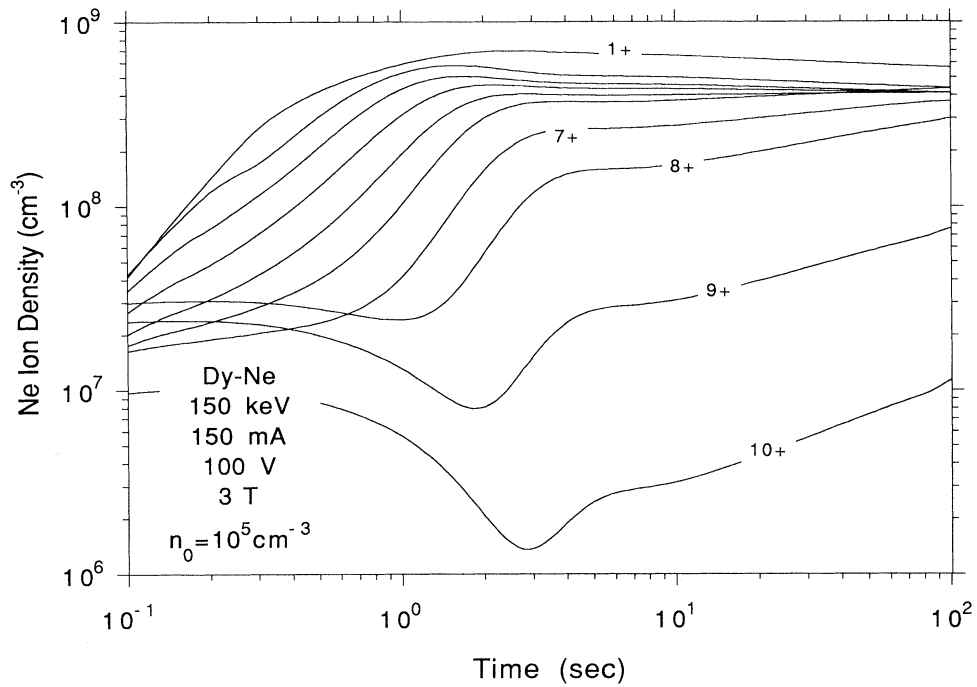


FIG. 11. Effect of a decreased axial potential well on the charge-state distributions of the neon coolant ions. The neutral neon density is 10^5 cm^{-3} and the initial total Dy ion density is 10^9 cm^{-3} . ($E_e = 150 \text{ keV}$, $I = 150 \text{ mA}$, $V_w = 100 \text{ V}$, $B = 3 \text{ T}$.)

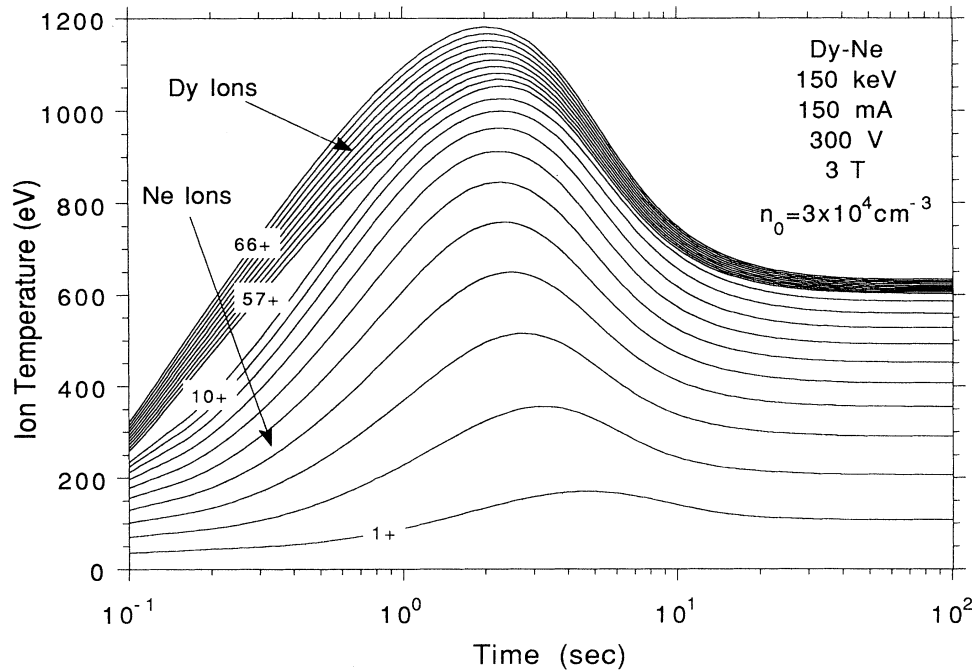


FIG. 12. Evolution of the ion temperatures for operating parameters optimum for cooling. The neutral neon density is $3 \times 10^4 \text{ cm}^{-3}$ and the initial total Dy ion density is 10^9 cm^{-3} . The applied axial potential is 300 V. ($E_e = 150 \text{ keV}$, $I = 150 \text{ mA}$, $B = 3 \text{ T}$.)

charge exchange and strongly affects the density of trapped Dy^{66+} . Our calculations are based on the Lotz formula.¹⁶ There is a paucity of ionization cross-section measurements at the energies of interest to check the accuracy of this formula. The measurements that do exist suggest that the ionization cross section for the production of the first few charge states could be two or three times larger than the Lotz value for gases heavier than neon. Thus the performance of aluminum as a coolant may have been underestimated in the present calculation.

Using an electron-beam ion source, Donets and Ovsyannikov²² made time-of-flight measurements of the evolution of ion charge-state distributions in a variety of gases. We suspect that in their experiment evaporative cooling was taking place because of the background gas and the continuous introduction of the source gas. Penetrante *et al.*¹⁵ have shown that with a continuous injection of the source gas into the EBIT, a form of evaporative cooling takes place in which the lower-charged coolant ions and the highly charged trapped ions are of the same gas species. By working at electron-beam currents for which the ion-loss rate is small (determined empirically by the rate of evolution of the charge distributions), Donets and Ovsyannikov²² were able to use a simple ionization kinetics model to derive the effective ionization cross sections for all ionization stages of C, N, O, and Ne, and some of the higher ionization stages of Ar. Their data are compared with the Lotz predictions in a compilation by Tawara and Kato.²³ For the highly charged Ar ions, their data show close agreement with the Lotz values.

In determining the charge exchange rate we have used the cross section formula of Müller and Salzborn.¹⁸ This empirical scaling formula was derived from measurements where the projectiles were Ne^{i+} , Ar^{i+} , Kr^{i+} , and Xe^{i+} and the targets were He, Ne, Ar, Kr, Xe, H_2 , N_2 , O_2 , CH_4 , and CO_2 . There are uncertainties as to the applicability of the formula outside the range of measurements. More experiments for slow highly charged ions would be valuable.

The selection of the coolant element is governed by other factors in addition to the effectiveness in cooling highly charged ions. These include vacuum and cryogenic characteristics, each of injection, and purity. The presence of heavy impurities could degrade the confinement of the highly charged Dy ions. Schneider *et al.*¹⁴ have done measurements of the containment time of Au^{69+} cooled by titanium. It was noted that the loss of the

highly charged gold ions was accompanied by an accumulation of lead in the trap. Lead is an impurity in commercial titanium. In that case lead ions were being trapped and cooled by both titanium ions and gold ions.

With a neon coolant, we found that the operating parameters for optimum cooling consist of an axial well depth of 300 V, a coolant density of around 10^4 cm^{-3} , and a total Dy ion density of 10^9 cm^{-3} . With these parameters the predicted steady-state temperature for the highly charged Dy ions is 600 eV, and the corresponding ion loss rates are negligible. The Dy ions consist of 7% Dy^{66+} . The exact values depend upon the quality of the collision cross sections.

VI. CONCLUSION

Evaporative cooling has been developed to overcome the limitations imposed by collisional heating on the maximum charge state and confinement time. It employs the continuous injection (and escape) of low-charged ions to cool the trapped highly charged ions. We have shown that neon is an ideal coolant for Dy^{66+} ions in the superEBIT. Significant amounts of bare and hydrogenlike Dy ions can be trapped indefinitely for the observation of bound-state β decay. The information we provide is valuable to other EBIT systems as well. There are two factors that dictate the choice of the coolant: (i) the effectiveness of the coolant in reducing the highly charged ion temperatures, and (ii) the degradation of the charge-state balance of the highly charged ions from charge exchange with the neutral component of the coolant. We have shown that neon, nitrogen, and helium have generally good coolant properties. The factor that determines the maximum amount of coolant is the neutralization of the electron beam space charge by the coolant ions. A "best" coolant can be chosen on the basis of better cross-section measurements and practical characteristics, i.e., purity, vacuum, and cryogenic properties, and ease of injection. We are confident that we can now determine an optimal cooling material for any highly charged ionization state desired in an electron-beam ion trap.

ACKNOWLEDGMENTS

This work was performed under the auspices of the U.S. Department of Energy by the Lawrence Livermore National Laboratory under Contract No. W-7405-ENG-48.

¹M. A. Levine, R. E. Marrs, J. R. Henderson, D. A. Knapp, and M. B. Schneider, *Phys. Scr.* **T22**, 157 (1988).

²M. A. Levine, R. E. Marrs, J. N. Bardsley, P. Beiersdorfer, C. L. Bennett, M. H. Chen, T. Cowan, D. Dietrich, J. R. Henderson, D. A. Knapp, A. Osterheld, B. M. Penetrante, M. B. Schneider, and J. H. Scofield, *Nucl. Instrum. Methods B* **43**, 431 (1989).

³R. E. Marrs, M. A. Levine, D. A. Knapp, and J. R. Henderson, *Phys. Rev. Lett.* **60**, 1715 (1988).

⁴D. A. Knapp, R. E. Marrs, M. A. Levine, C. L. Bennett, M. H.

Chen, J. R. Henderson, M. B. Schneider, and J. H. Scofield, *Phys. Rev. Lett.* **62**, 2104 (1989).

⁵P. Beiersdorfer, R. E. Marrs, J. R. Henderson, D. A. Knapp, M. A. Levine, D. B. Platt, M. B. Schneider, D. A. Vogel, and K. L. Wong, *Rev. Sci. Instrum.* **61**, 2338 (1990).

⁶R. E. Marrs, C. Bennett, M. H. Chen, T. Cowan, D. Dietrich, J. R. Henderson, D. A. Knapp, M. A. Levine, K. J. Reed, M. B. Schneider, and J. H. Scofield, *J. Phys. (Paris) Colloq.* **50**, C1-445 (1989).

⁷C. M. Brown, U. Feldman, G. A. Doschek, J. F. Seely, R. E.

- LaVilla, V. L. Jacobs, J. R. Henderson, D. A. Knapp, R. E. Marrs, P. Beiersdorfer, and M. A. Levine, *Phys. Rev. A* **40**, 4089 (1989).
- ⁸P. Beiersdorfer, M. H. Chen, R. E. Marrs, and M. A. Levine, *Phys. Rev. A* **41**, 3453 (1990).
- ⁹P. Beiersdorfer, A. L. Osterheld, M. B. Schneider, W. Goldstein, J. R. Henderson, D. A. Knapp, M. A. Levine, R. E. Marrs, and D. Vogel, *Phys. Rev. Lett.* **65**, 1995 (1990).
- ¹⁰J. R. Henderson, P. Beiersdorfer, C. L. Bennett, S. Chantrenne, D. A. Knapp, R. E. Marrs, M. B. Schneider, K. L. Wong, G. A. Doschek, J. F. Seely, C. M. Brown, R. E. LaVilla, J. Dubau, and M. A. Levine, *Phys. Rev. Lett.* **65**, 705 (1990).
- ¹¹D. A. Knapp, C. L. Bennett, J. R. Henderson, R. E. Marrs, and M. B. Schneider, *Bull. Am. Phys. Soc.* **34**, 1394 (1989).
- ¹²K. Takahashi and K. Yokoi, *Nucl. Phys. A* **404**, 578 (1983).
- ¹³I. G. Brown, J. E. Galvin, R. A. MacGill, and R. T. Wright, *Appl. Phys. Lett.* **49**, 1019 (1986).
- ¹⁴M. B. Schneider, M. A. Levine, C. L. Bennett, J. R. Henderson, D. A. Knapp, and R. E. Marrs, in *International Symposium on Electron Beam Ion Sources and Their Applications*, Proceedings of the International Symposium held on Electron Beam Ion Sources and their Applications at the Brookhaven National Laboratory, Upton, 1988, AIP Conf. Proc. No. 188, edited by A. Hershcovitch (AIP, New York, 1989), p. 158.
- ¹⁵B. M. Penetrante, J. N. Bardsley, D. DeWitt, M. Clark, and D. Schneider, preceding paper, *Phys. Rev. A* **43**, 4861 (1991).
- ¹⁶W. Lotz, *Z. Phys.* **206**, 205 (1967); **216**, 241 (1968).
- ¹⁷Y. S. Kim and R. H. Pratt, *Phys. Rev. A* **27**, 2913 (1983).
- ¹⁸A. Müller and E. Salzborn, *Phys. Lett.* **62A**, 391 (1977).
- ¹⁹I. P. Shkarofsky, T. W. Johnston, and M. P. Bachynski, *The Particle Kinetics of Plasmas* (Addison-Wesley, Reading, MA, 1966).
- ²⁰L. Spitzer, *Physics of Fully Ionized Gases* (Interscience, New York, 1956).
- ²¹V. P. Pastukhov, *Nucl. Fusion* **14**, 3 (1974).
- ²²E. D. Donets and V. P. Ovsyannikov, *Zh. Eksp. Teor. Fiz.* **80**, 916 (1981) [*Sov. Phys.—JETP* **53**, 466 (1981)].
- ²³H. Tawara and T. Kato, *At. Data Nucl. Data Tables* **36**, 167 (1987).